Available online at www.sciencedirect.com
SCIENCE DIRECT®
Journal of Molecular Catalysis A: Chemical 231 (2005) 113–122
JOURNAL OF MOLECULAR CATALYSIS A: CHEMICAL
www.elsevier.com/locate/molcata

Catalytic reactions of post-consumer polymer waste over fluidised cracking catalysts for producing hydrocarbons

Y.-H. Lin*, M.-H. Yang

Department of Biochemical Engineering and Graduate Institute of Environmental Polymeric Materials, Kao Yuan Institute of Technology, 821, Kaohsiung, Taiwan, ROC

Received 26 November 2004; received in revised form 31 December 2004; accepted 2 January 2005
Available online 2 February 2005

Abstract

A post-consumer polymer mixture (PE/PP/PS/PVC) was pyrolysed over catalysts using a laboratory fluidised-bed reactor operating isothermally at ambient pressure. The effects of reaction conditions including catalyst, temperature, ratios of commingled polymer to catalyst feed and flow rates of fluidising gas were examined. The yield of volatile hydrocarbons for zeolitic catalysts (HZSM-5 > HUSY ≈ HMOR) gave higher yield than non-zeolitic catalysts (SAHA ≈ MCM-41). Product distributions with HZSM-5 contained more olefinic materials with about 60 wt.% in the range of C_3–C_5. However, both HMOR and HUSY produced more paraffinic streams with large amounts of butane (C_4). The larger pore zeolites (HUSY and HMOR) showed deactivation in contrast to the more restrictive HZSM-5. MCM-41 and SAHA showed the lowest conversion and generated an olefin-rich product with a rise to the broadest carbon range of C_3–C_7. The selectivity could be further influenced by changes in reactor conditions. Valuable hydrocarbons of olefins and *iso*-olefins were produced by low temperatures and short contact times used in this study.

Keywords: Polymer waste; Pyrolysis; Fluidised-bed reactor; Catalysts; Selectivity

1. Introduction

The disposal problem of municipal solid waste (MSW) or industrial waste materials has become an increasingly intricate and costly event because of the decrease in space available for landfills and the growing concern about living environment. Among these materials, the percentage of plastic of MSW was tremendous and expected to increase year by year [1]. Large amounts of waste plastics are still treated by landfilling or incineration, since the cost of feedstock recycling is highest for waste plastic treatment [2]. In view of their biodegradability, most polymers are felt unsuitable for landfill disposal. The destruction of wastes by incineration is prevalent, but this practice is expensive and often generates problems with unacceptable emissions. Methods for recycling plastic waste have been developed and new recycling approaches are being investigated [3]. Chemical recycling, i.e., conversion of waste polymers into feedstock or fuels, has been recognised as an ideal approach and could significantly reduce the net cost of disposal [4].

Possible technologies for the conversion of polymer waste to useful products have attracted research in the area of thermal degradation. Workers have developed a dual fluidised-bed process for obtaining medium quality gases from municipal solid waste [5–7]. Thermal cracking of waste polymer using kilns or fluid beds has been piloted on a significant scale [8–10]. However, the thermal degradation of polymers to low molecular weight materials has a major drawback in that a very broad product range is obtained. In addition,

* Corresponding author. Tel.: +886 7 6077777; fax: +886 7 6077788.
E-mail address: lin@cc.kyit.edu.tw (Y.-H. Lin).

1381-1169/$ – see front matter © 2004 Elsevier B.V. All rights reserved.
doi:10.1016/j.molcata.2005.01.003

Table 1
Catalysts used in fluidised-bed reactor for commingled polymer (CP#5) degradation

Catalyst	Micropore size (nm)	BET area (cm^3/g)	Si/Al ratio	Commercial name
HUSY	0.74	603	6.0	H-ultrastabilised Y zeolite[a]
HZSM-5	0.55 × 0.51	391	17.1	HZSM-5 zeolite[b]
HMOR	0.65 × 0.70	561	6.3	H-mordenite[c]
SAHA	3.15[d]	274	2.6	Synclyst 25[a] (silica–alumina)
MCM-41{Al}	4.2–5.2[d]	845	17.5	–[e]

[a] Crosfield Chemicals, Warrington, UK.
[b] BP Chemicals, Sunbury-on-Thames, UK.
[c] Laporte, Warrington, UK.
[d] Single point BET determination.
[e] Synthesised by procedure outlined by Beck [25].

these processes require high temperatures, typically more than 500 °C and even up to 900 °C. Catalytic pyrolysis provides a means to address these problems. The addition of catalyst is expected to reduce decomposition temperature, to promote decomposition speed, and to modify the products [11–16]. Catalytic pyrolysis has been carried out by considering a variety of catalysts with little emphasis on the reactor design, with only simple adiabatic batch and fixed bed reactors being used [17–20]. However, the use of fixed beds or adiabatic batch where polymer and catalyst are contacted directly leads to problems of blockage and difficulty in obtaining intimate contact over the whole reactor. Without good contact the formation of large amounts of residue are likely, and scale-up to industrial scale is not feasible [21–23].

Much less is known about performance of catalyst in polymer degradation using a fluidised-bed reactor. Also, most studies have mainly concentrated on the catalytic pyrolysis of pure polymers [11–20,22–24]. A more difficult task is recycling of post-consumer municipal plastic waste since it consists of not only hydrocarbons but also nitrogen and sulphur-containing mixed polymers as well as some modified materials. The objective of this current work is to explore the capabilities of a catalytic fluidised-bed reaction system using various cracking catalysts (i) for the study of product distribution and selectivity on the catalytic degradation of commingled post-consumer plastic and (ii) for identification of suitable reaction conditions for achieving waste polymer recycling.

2. Experimental

2.1. Materials and reaction preparation

The commingled polymer (CP#5) used in this study was obtained from post-consumer plastic waste streams of several communities in South-Taiwan named as Kaohsiung Plastic Recycling Center (KPRC) with the component of PE (∼62 wt.% = ∼38 wt.% HDPE + ∼24 wt.% LDPE), PP (∼30 wt.%), PS (∼7 wt.%) and with about 1 wt.% PVC mixtures. Typically, the content of waste plastic sample tested by ultimate analysis was about 86.24% C, 12.95% H, 0.56% Cl, 0.05% O, 0.07% N, and 0.13% S. The catalysts employed are described in Table 1. Prior to use, all the catalysts were pelleted, crushed and sieved to give particle sizes ranging from 75 to 180 μm. The catalyst (0.2–0.3 g) was then activated by heating in the reactor in flowing nitrogen (50 ml min^{-1}) to 120 °C at 60 °C h^{-1}. After 2 h the temperature was increased to 520 °C at a rate of 120 °C h^{-1}. After 5 h at 520 °C the reactor was cooled to the desired reaction temperature. Several fluidisation runs were performed at ambient temperature and pressure to select suitable particle sizes (both catalyst and polymer) and to optimise the fluidising gas flow rates to be used during the reaction. The particle sizes of both catalyst (75–180 μm) and polymer (75–250 μm) were chosen as being large enough to avoid entrainment but not too large to be inadequately fluidised.

2.2. Experimental procedures and product analysis

A process flow diagram of the experimental system is given elsewhere [26] and shown schematically in Fig. 1. The reactor consists of a pyrex glass tube (170 mm × 20 mm i.d., an upper section; 30 mm × 10 mm i.d., a middle section; 200 mm × 10 mm i.d., a lower section) with a sintered distributor (10 mm i.d., in the middle section) and a three-zone heating furnace with digital controllers. High-purity nitrogen was used as the fluidising gas and the flow was controlled by a needle valve. The polymer feed system was designed to allow commingled polymer (CP#5) particles, purged under nitrogen, to enter the top of the reactor and to drop freely into the fluidised-bed at $t = 0$ min. The added polymer melts, wets the catalyst surface and is pulled into the catalyst macropores by capillary action [27]. At sufficiently low polymer/catalyst ratios the outside of the catalyst particles are not wet with polymer, so the catalyst particles move freely.

Volatile products leaving the reactor were passed through a glass-fibre filter to capture catalyst fines, followed by an ice-acetone condenser (the ice-water and acetone was used and gave an approximate temperature of −15 °C) to collect any condensible liquid product. A de-ionised water trap was placed in series after the condenser to catch any HCl produced by the degradation of PVC component. A three-way valve was used after the condenser to route product either

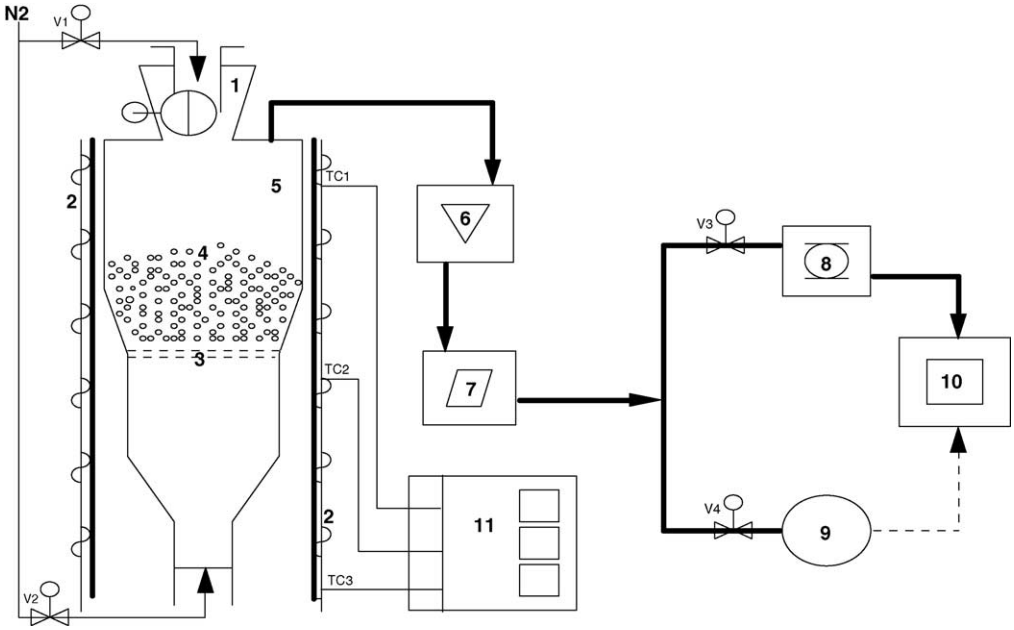

Fig. 1. Schematic diagram of a catalytic fluidised-bed reactor system: (1) feeder, (2) furnace, (3) sintered distributor, (4) fluidised catalyst, (5) reactor, (6) condenser, (7) de-ionised water trap, (8) 16-loop automated sample system, (9) gas bag, (10) GC, (11) digital controller for three-zone furnace.

into a sample gas bag or to an automated sample valve system with 16 loops. The Tedlar bags, 15 l capacity, were used to collect time-averaged gaseous samples. The bags were replaced at intervals of 10 min throughout the course of reaction. The multiport sampling valve allowed frequent, rapid sampling of the product stream when required. Spot samples were collected and analysed at various reaction times (t = 1, 2, 3, 5, 8, 12,15, 20 min). The rate of hydrocarbon production (R_{gp}, wt.% min^{-1}) was defined by the relationship: R_{gp} = hydrocarbon production rate (g/min) × 100/total hydrocarbon product over the whole run (g).

Gaseous hydrocarbon products were analysed using a gas chromatograph equipped with (i) a thermal conductivity detector (TCD) fitted with a 1.5 m × 0.2 mm i.d. Molecular Sieve 13X packed column and (ii) a flame ionisation detector (FID) fitted with a 50 m × 0.32 mm i.d. PLOT Al_2O_3/KCl capillary column. A calibration cylinder containing 1% C_1–C_5 hydrocarbons was used to help identify and quantify the gaseous products. The HCl in de-ionised water samples were analysed using a Corning pH/ion meter with a chloride electrode calibrated between 100 and 1000 ppm. A double junction reference electrode filled with KNO_3 with a fixed potential was used in conjunction with the chloride. The solid remaining deposited on the catalyst after the catalytic degradation of the polymer were deemed "residues" and contained involatile products and coke. The amount and nature of the residues was determined by thermogravimetric analysis as described elsewhere [27]. Data analysis was carried out using a Microsoft Excel spreadsheet. The reactor and various units of the collection system were weighted before and after the runs to determine the mass balance.

3. Results and discussion

Catalytic pyrolysis products (P) are grouped together as hydrocarbon gases (<C_5), gasoline up to C_9 (C_5–C_9), liquids (condensate in condenser and filter), HCl (trapped in de-ionised solution) and residues (coke and products, involatile at reaction temperature, deposited on catalyst) to enable the overall pyrolysis processes to be described more easily. A number of runs were repeated in order to check their reproducibility. It was found that the experimental error was within ±5%. The term "yield" as used in this paper is defined by the relationshipyield (wt.%) = (P (g) × 100)/polymer fed (g).

Due to the high nitrogen flow rates used in this study, it is difficult to completely recover all the lower molecular weight material, and this results in some loss in the mass balance. Mass balances of 90 ± 5% were obtained for all experiments.

3.1. Degradation of commingled polymer over various catalysts

The reaction yield (based on the feed) of commingled polymer (CP#5) degradation for each catalyst is summarised in Table 2. The yield of volatile hydrocarbons for zeolitic catalysts (HZSM-5 > HUSY ≈ HMOR) gave higher yield than non-zeolitic catalysts (SAHA ≈ MCM-41) and the highest yield (nearly 90 wt.%) was obtained for HZSM-5. Overall, the bulk of the products observed were in the gas phase with less than 7 wt.% liquid collected. The highest level of unconverted polymer was observed with SAHA and MCM-41, while the highest coke yields were observed with HUSY and HMOR. Some similarities were observed between HZSM-5 and HMOR with C_1–C_4 and C_5–C_9 yields, which were

Table 2
Product distributions for the degradation of CP#5 polymer over various cracking catalysts (reaction temperature = 360 °C, fluidising N_2 rate = 570 ml min^{-1}, polymer to catalyst ratio = 40% (wt/wt), and total time of collection = 30 min)

Degradation results	Catalyst type				
	HZSM-5	HUSY	HMOR	SAHA	MCM-41
Yield (wt.% feed)					
Gaseous	90.65	87.51	86.63	83.56	84.15
Liquid[a]	3.71	4.03	4.55	6.43	5.11
Residue[b]	5.12	7.92	8.33	9.56	10.23
Involatile residue	3.43	4.27	5.22	7.93	7.31
Coke	1.69	3.75	3.11	2.63	2.92
HCl	0.52	0.54	0.49	0.45	0.51
Mass balance (%)	93.15	90.56	93.68	88.68	89.41
Distribution of gaseous products (wt.% feed)					
Hydrocarbon gases ($\sum C_1$–C_4)	56.37	31.64	51.58	25.34	27.31
C_1	0.06	–[c]	–[c]	n.d.[d]	n.d.[d]
C_2	0.54	0.02	0.14	–[c]	–[c]
$C_2^=$	2.17	0.21	0.68	0.12	0.03
C_3	2.87	0.48	2.47	1.03	0.61
$C_3^=$	19.35	8.14	14.13	6.32	5.15
C_4	9.53	12.65	16.54	1.59	1.90
$C_4^=$	21.85	10.14	17.62	16.28	19.62
Gasoline ($\sum C_5$–C_9)	34.28	50.84	35.95	53.71	56.84
C_5	4.82	13.68	7.20	2.26	1.53
$C_5^=$	11.63	7.44	10.73	17.23	19.37
C_6	3.19	12.36	3.45	3.36	3.17
$C_6^=$	4.18	4.25	4.41	12.88	10.65
C_7	2.52	8.63	0.85	4.34	4.51
$C_7^=$	1.47	2.72	1.03	5.30	6.13
C_8	0.39	5.14	0.37	1.03	2.68
$C_8^=$	0.21	1.03	0.83	1.01	2.24
$\sum C_9$	0.06	0.56	0.25	0.81	1.31
Styrene	4.15	4.21	3.87	5.23	5.11
BTX[e]	1.66	0.82	1.96	0.26	0.14

[a] Liquid: condensate in condenser and captured in filter.
[b] Residue: coke and involatile products.
[c] Less than 0.01 wt.%.
[d] Not detectable.
[e] BTX: benzene, toluene and xylene.

approximately 52–56 and 34–35 wt.%, respectively. However, with SAHA and MCM-41 the C_1–C_4 and C_5–C_9 yields were approximately 25–27 and 54–57 wt.%, respectively.

The individual volatile hydrocarbon products of CP#5 degradation over various catalysts are also listed in Table 2. Product distributions with HZSM-5 contained more olefinic materials with about 60 wt.% in the range of C_3–C_5. The results of the products of CP#5 degradation reflect the differing cracking effect of the zeolite compared with the non-zeolitic materials. Zeolites (HUSY, HZSM-5 and HMOR) produced more paraffinic streams with large amounts of butanes (C_4). The differences in the product distributions between the zeolites can be seen with HUSY producing a wider molecular weight range than HZSM-5 and HMOR. HMOR was particularly selective to C_4 products generating over 34 wt.%. Both SAHA and MCM-41 resulted in a highly olefinic product with the stylene component and gave rise to the broadest carbon range of C_3–C_7. The rate of gaseous hydrocarbon evolution further highlights the slower rate of degradation over non-zeolitic catalysts (SAHA and MCM-41) as shown in Fig. 2 when comparing all catalysts under identical conditions at

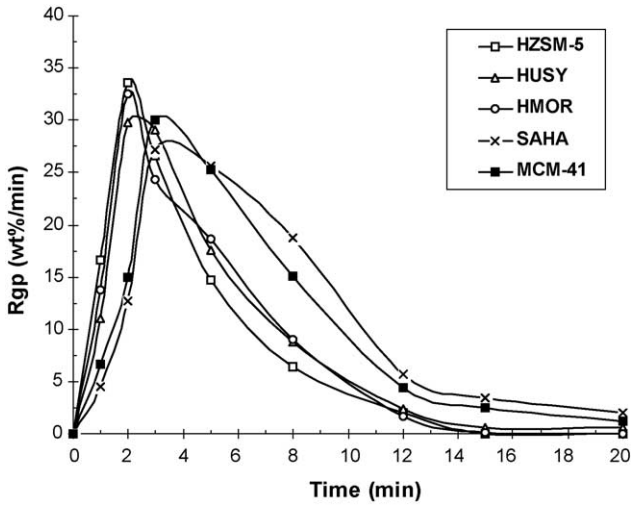

Fig. 2. Comparison of olefinic products for the catalytic degradation of commingled polymer (CP#5) at 360 °C over different catalysts (polymer to catalyst ratio = 40% (wt/wt), rate of fluidisation gas = 570 ml min^{-1}).

360 °C. The maximum rate of generation was observed after 2 min with the zeolite catalysts whereas the maximum was observed after 3 min with SAHA and MCM-41.

3.2. Influence of operating conditions on commingled polymer degradation

The influence of operation conditions including temperature (290–430 °C), flow rates of fludising gas (270–900 ml min^{-1}), and ratios of commingled polymer (CP#5) to catalyst feed (0.1:1 to 1:1) has been investigated in this paper. Some similar trends in product yields were observed with HZSM-5 as the reaction temperature was increased. Gaseous and coke yields increased and involatile residues (unreacted or partially reacted CP#5) and liquids decreased (Table 3). The rate of hydrocarbon production as a function of time for CP#5 degradation over HZSM-5 at different reaction temperatures is compared in Fig. 3 and, as expected, faster rates were observed at higher temperatures. At 430 °C, the maximum rate of hydrocarbon production was 44 wt.% min^{-1} after only 1 min with all the polymer degraded after approximately 5 min. As the temperature of reaction was decreased, the initial rate of hydrocarbon production dropped and the time for CP#5 polymer to be degraded lengthened. At 290 °C the rate of hydrocarbon production was significantly lower with the polymer being degraded more slowly over 20 min. The change in the hydrocarbon yield with temperature was similar, for all catalysts used, with faster rates observed at higher temperatures.

The results shown in Fig. 4 illustrate that for efficient commingled polymer (CP#5) degradation good mixing is required, with a dramatic drop-off in the rate of degradation observed only at the lowest fluidising flow used (270 ml min^{-1}).

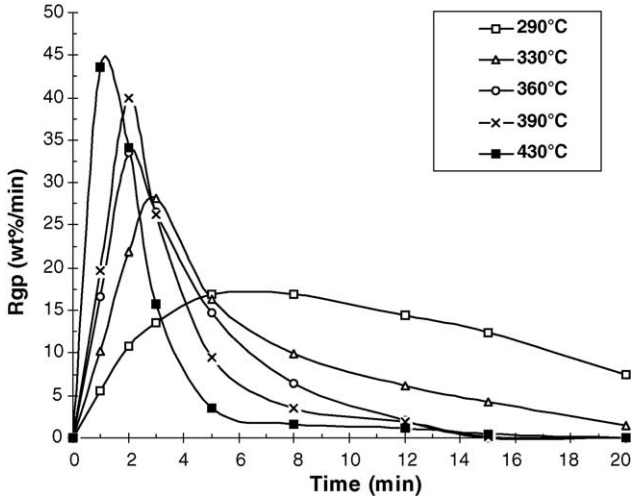

Fig. 3. Comparison of hydrocarbon yields as a function of time at different reaction temperatures for the degradation of CP#5 polymer over HZSM-5 (rate of fluidisation gas = 570 ml min^{-1}, catalyst particle size = 75–180 μm, polymer to catalyst ratio = 40 wt.%).

Furthermore, changing the fluidising flow rate influences the product distribution. At low flow rates (longer contact times), secondary products are observed with increased amounts of coke precursors (BTX) although the overall degradation rate is slower as shown by increasing amounts of partially depolymerised products (Table 4). The amount of catalyst used in the degradation of CP#5 remained constant and, therefore, as more polymers was added to the reactor then fewer catalytic sites per unit weight of catalyst were available for cracking. The overall effect of increasing the polymer to catalyst ratio from 1:10 to 1:1 on the rate of hydrocarbon generation was small but predictable (Fig. 5). As the polymer to catalyst ratio increases, the possibility of CP#5 adhesion to the reactor wall

Table 3
Product distributions shown from HZSM-5 catalysed pyrolysis of CP#5 polymer at different reaction temperatures (fluidising N_2 rate = 570 ml min^{-1}, catalyst particle size = 75–180 μm, and polymer to catalyst ratio = 40 wt.%)

Degradation results	Temperature (°C)				
	290	330	360	390	430
Total time of collection (min)	40	30	20	20	20
Yield (wt.% feed)					
Gaseous	86.36	88.44	90.65	91.20	92.12
Liquid[a]	5.31	4.19	3.71	3.36	3.22
Residue[b]	8.33	6.83	5.12	4.91	4.14
Involatile residue	6.96	5.29	3.43	3.07	2.17
Coke	1.37	1.58	1.69	1.84	1.97
HCl	0.48	0.54	0.52	0.53	0.52
Mass balance (%)	89.32	91.17	93.15	94.18	92.73
Distribution of gaseous products (wt.% feed)					
Hydrocarbon gases ($\sum C_1$–C_4)	52.04	54.41	56.37	60.95	61.34
Gasoline ($\sum C_5$–C_9)	34.32	34.03	34.28	30.25	30.78
Styrene	4.71	4.26	4.15	4.23	4.11
BTX[c]	1.13	1.44	1.66	1.76	1.83

[a] Liquid: condensate in condenser and captured in filter.
[b] Residue: coke and involatile products.
[c] BTX: benzene, toluene and xylene.

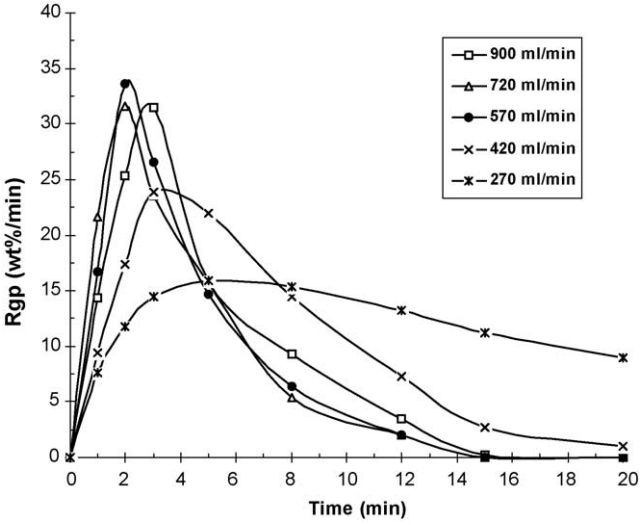

Fig. 4. Comparison of hydrocarbon yields as a function of time at different fluidisation gas for the degradation of CP#5 polymer over HZSM-5 (reaction temperature = 360 °C, catalyst particle size = 75–180 μm, polymer to catalyst ratio = 40 wt.%).

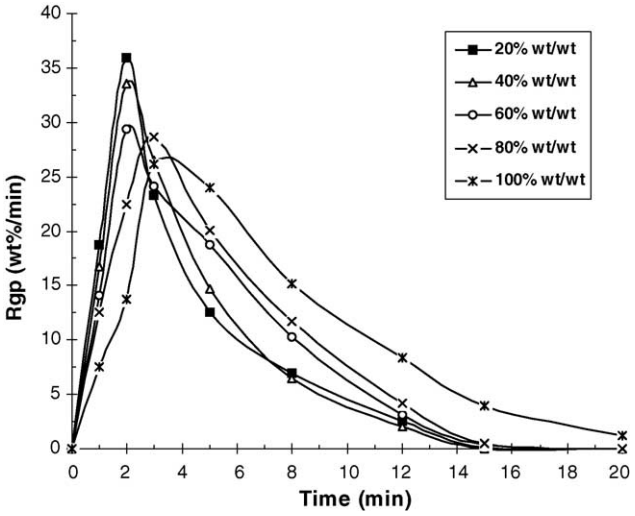

Fig. 5. Comparison of hydrocarbon yields as a function of time at different ratios of polymer to catalyst for the degradation of CP#5 polymer over HZSM-5 (reaction temperature = 360 °C, catalyst particle size = 75–180 μm, rate of fluidisation gas = 570 ml min^{-1}).

increases as the amount of unreacted polymer in the reactor rises. However, for the work carried out in this paper no such problems were observed. Also, the maximum rate observed dropped slightly and the time taken to generate the maximum rate extended from 2 to 3 min. The total product yield after 15 min showed only a slight downward trend even after a 10-fold increase in added polymer. This can be attributed to the high activity of HZSM-5 and excellent contact between CP#5 polymer and catalyst particles. Consequently, as more CP#5 was added, lower C_1–C_4 hydrocarbon gases yields but higher liquid yields and involatile products were observed. In addition, more BTX (coke precursor) was produced but increasing the polymer to catalyst ratio had only virtually no effect on gasoline production (Table 5).

3.3. Product stream variation with catalyst deactivation and reaction conditions

The relation in catalytic activity to catalyst deactivation was examined by the transient change in the amount of gaseous compounds produced. Rapid variation in the product stream of both zeolite catalysts (HUSY and HMOR) and MCM-41 was observed (Fig. 6) when the spot samples, taken during the course of the reaction, were analysed. The deactivation is reflected in the decrease of the amount of *iso*-butane (*i*-C_4) and *iso*-pentane (*i*-C_5) produced (product of bimolecular reaction) and the relative increase in olefins (product of monomolecular reaction), exemplified by, $C_4^=$ and $C_5^=$. HZSM-5 and SAHA product streams

Table 4
Product distributions shown from HZSM-5 catalysed pyrolysis of CP#5 polymer at different fluidising N_2 rates (reaction temperature = 360 °C, catalyst particle size = 75–180 μm, polymer to catalyst ratio = 40 wt.%, and total time of collection = 20 min)

Degradation results	Fluidising N_2 rates (ml min^{-1})				
	900	720	570	420	270
Yield (wt.% feed)					
Gaseous	88.14	89.36	90.65	91.23	90.28
Liquid[a]	5.84	4.81	3.71	3.13	3.03
Residue[b]	5.53	5.34	5.12	5.64	6.11
Involatile residue	4.35	3.90	3.43	4.01	3.69
Coke	1.18	1.44	1.69	1.63	1.72
HCl	0.49	0.49	0.52	0.56	0.59
Mass balance (%)	91.46	89.47	93.15	93.62	92.71
Distribution of gaseous products (wt.% feed)					
Hydrocarbon gases ($\sum C_1$–C_4)	55.35	55.36	56.37	57.42	58.83
Gasoline ($\sum C_5$–C_9)	32.79	34.00	34.28	33.81	31.45
Styrene	4.15	4.02	4.15	4.32	4.26
BTX[c]	0.72	1.13	1.66	1.91	2.31

[a] Liquid: condensate in condenser and captured in filter.
[b] Residue: coke and involatile products.
[c] BTX: benzene, toluene and xylene.

Table 5
Product distributions shown from HZSM-5 catalysed pyrolysis of CP#5 polymer at different ratios of polymer to catalyst (reaction temperature = 360 °C, catalyst particle size = 75–180 μm, fluidising N_2 rate = 570 ml min^{-1}, and total time of collection = 20 min)

Degradation results	Ratio of polymer to catalyst (wt.%)				
	10	20	60	80	100
Yield (wt.% feed)					
Gaseous	92.08	91.62	89.20	88.03	87.51
Liquid[a]	3.10	3.43	3.82	4.64	4.77
Residue[b]	4.26	4.43	6.44	6.84	7.13
Involatile residue	2.68	2.70	4.85	5.16	5.31
Coke	1.58	1.73	1.59	1.68	1.82
HCl	0.56	0.52	0.54	0.49	0.59
Mass balance (%)	88.32	91.43	91.82	92.54	92.39
Distribution of gaseous products (wt.% feed)					
Hydrocarbon gases ($\sum C_1$–C_4)	59.62	58.13	55.56	54.17	51.46
Gasoline ($\sum C_5$–C_9)	32.46	33.49	33.64	33.86	36.05
Styrene	4.93	4.81	4.15	4.04	4.45
BTX[c]	1.37	1.46	1.63	2.30	2.53

[a] Liquid: condensate in condenser and captured in filter.
[b] Residue: coke and involatile products.
[c] BTX: benzene, toluene and xylene.

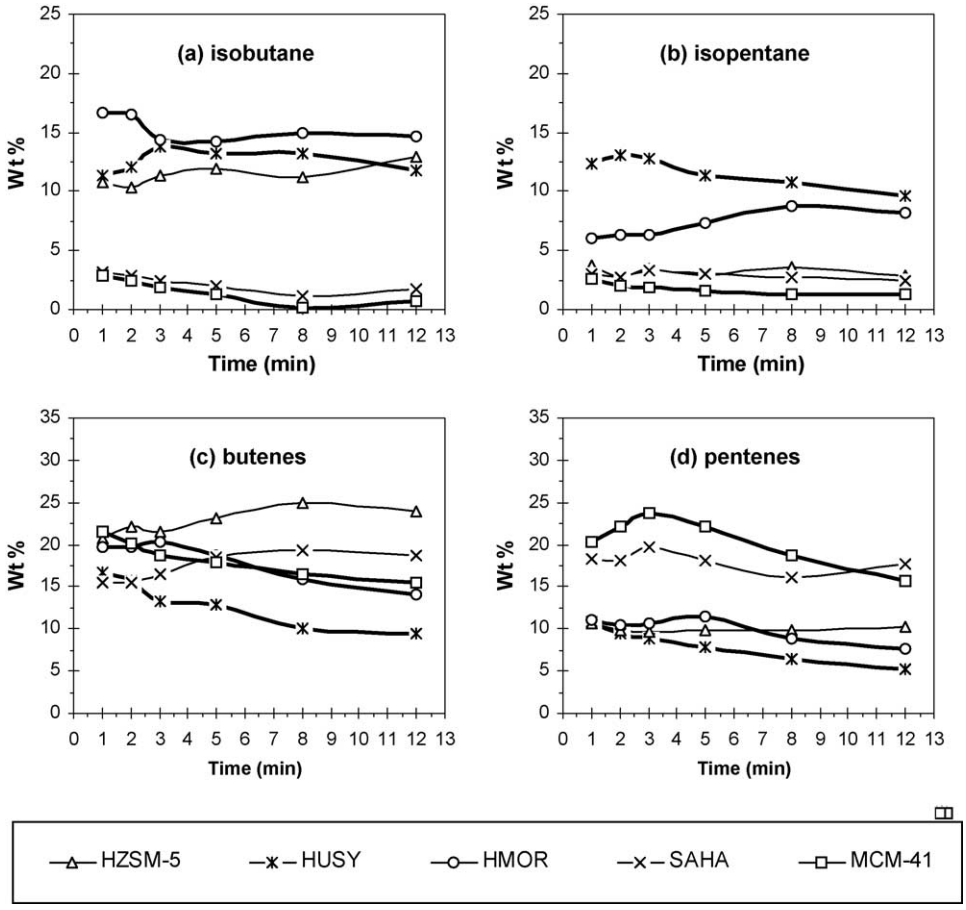

Fig. 6. Comparison of some of the main hydrocarbon products ((a) *iso*-butane; *i*-C_4, (b) butenes, $\sum C_4^=$ (c) *iso*-pentane; *i*-C_5 and (d) pentenes; $\sum C_5^=$) as a function of time for the degradation of CP#5 polymer over different catalysts (reaction temperature = 360 °C, rate of fluidisation gas = 570 ml min^{-1}, catalyst particle size = 75–180 μm, polymer to catalyst ratio = 40 wt.%).

remain virtually unchanged throughout the degradation of commingled polymer (CP#5). HZSM-5 is resistant to coking when coke builds up on outersurface and the product stream remains essentially unchanged, whereas the weakness and lower density of the acid sites in SAHA along with the increased tolerance to coke in the amorphous structure is most likely the reason for the lack of variation in the product stream over this catalyst. Both acidity and diffusion constraints within individual micropores of each catalyst may play significant roles in the observed product distribution. The systematic experiments discussed in this work and in earlier work [28] indicate that catalyst deactivation is being produced by active-site coverage, and consequently decrease the activity of the catalyst, giving the reason of decreasing of reaction rate with reaction time.

Equilibrium ratios of *i*-butane/*n*-butane and *i*-butene /$\sum$ butenes were predicted using Gibbs free energy minimisation on the PRO/II package for the temperatures used experimentally and are presented alongside the corresponding experimental results in Table 6. The *i*-butene/$\sum$ butenes ratio is very close to the predicted equilibrium values and thus the reactions involved in the production and interconversion of butenes are very fast over zeolitic catalysts, and their ratio is primarily equilibrium controlled. The *i*-butane/*n*-butane ratio reflects the involvement of tertiary C_4 carbenium ions in bimolecular hydrogen transfer reactions and since tertiary carbenium ions are more stable than primary ions, a higher yield of *iso*-butane would be expected. As can be seen in Table 6, the observed *i*-C_4/*n*-C_4 ratios at 360 °C are well above calculated equilibrium values and are consistent with the steric constraints of their structures following the order HZSM-5 (*i*-C_4/*n*-C_4 = 3.27) < HUSY (*i*-C_4/*n*-C_4 = 6.83) < HMOR (*i*-C_4/*n*-C_4 = 8.12).

Both the carbon number distribution of the products of CP#5 polymer cracking at 360 °C over the various catalysts used in this study and the nature of the product distribution were found to vary with the catalyst used. The less acidic amorphous SAHA and larger mesopores MCM-41 catalysts resulted in a highly olefinic product ($\sum$ olefin/ $\sum$ paraffin (o/p) = 4.18 and 4.02) and the largest amount of involatile residue (7.93 and 7.31 wt.%, see Table 2). By comparison, the stronger acid sites of the zeolite catalysts resulted in increased bimolecular hydrogen transfer following the order HZSM-5 (o/p = 2.54) < HMOR (o/p = 1.58) < HUSY (o/p = 0.63). Bimolecular reactions, such as hydrogen transfer, are sterically hindered within the 10 ring channel system of HZSM-5. However, the 12 ring channels of HMOR are less restrictive; hence the increase in the paraffin product. The combination of 12 ring pore openings and large internal supercages of HUSY allow significant bimolecular reactions and yielded a saturate-rich product. The selectivity could be varied by changes in different operating conditions used in this study. The yield of smaller cracked products increased with temperature as did the yields of coke and BTX (Table 3). Further evidence of the increase in secondary reactions was seen in the lowering of the *i*-C_4/*n*-C_4 and o/p ratios with temperature (Table 6). The pore structure of HZSM-5 restricts the formation of bulky intermediates and consequently the catalyst is resistant to coke formation explaining the relatively low values observed at high conversions and the very small increase with increasing reaction temperature. At fast flow rates (short contact times), primary cracking products are favoured as evidenced by the increasing ratios of *i*-butene/$\sum$ butenes (*i*-C_4/*n*-C_4 = 3.02 in 270 ml min^{-1} N_2 fluidising rate versus *i*-C_4/*n*-C_4 = 4.65 in 900 ml min^{-1} N_2 fluidising rate) and $\sum$olefin/$\sum$paraffin (o/p = 2.37 in 270 ml min^{-1} N_2 fluidising rate versus o/p = 3.04 in 900 ml min^{-1} N_2 fluidising rate).

3.4. Discussion

To convert post-consumer polymer waste, which contained mostly polyolefins (PE, PP and PS) and minor amounts of heteroatoms (S, Cl), the concentration of chlorine and sulphur containing components is important for further

Table 6
Influence of reaction conditions on product selectivity for the catalysed degradation of CP#5 polymer: experimental and predicted equilibrium results

Ratio	Reaction conditions													
	Catalyst type[a]					Temperature[b] (°C)			P/C ratio[c] (wt.%)			N_2 rate[d] (ml min^{-1})		
	ZSM-5	HUSY	HMOR	SAHA	MCM-41	290	360	430	10	60	100	270	570	900
i-butene/$\sum$ butenes	0.51	0.54	0.62	0.57	0.65	0.56	0.51	0.44	0.57	0.52	0.54	0.44	0.51	0.55
i-butene/$\sum$ butenes[e]						0.56	0.52	0.48						
i-butane/*n*-butane	3.27	6.83	8.12	2.19	5.71	5.38	3.27	2.46	3.72	3.41	3.66	3.02	3.41	4.65
i-butane/*n*-butane[e]						1.17	0.95	0.81						
$\sum$ olefins / $\sum$ paraffins[f]	2.54	0.63	1.58	4.18	4.02	3.12	2.54	2.16	2.91	2.54	2.66	2.21	2.54	3.04

[a] Represents a series of runs where reaction temperature = 360 °C, 40 wt/wt commingled polymer mixture to catalyst feed and 570 ml min^{-1} N_2 fluidising rate.
[b] Polymer mixture to catalyst ratio = 40 wt.% and 570 ml min^{-1} N_2 fluidising rate.
[c] Reaction temperature = 360 °C and fluidising N_2 = 570 ml min^{-1}.
[d] Polymer mixture to catalyst ratio = 40 wt.% and reaction temperature = 360 °C.
[e] Predicted equilibrium data.
[f] Denotes the ratio of the sum all olefinic to paraffinic products.

application. The chlorine was chemically separated from the PVC component and as a hydrochloric acid (HCl) in deionised water system. Similar trends in volatile hydrocarbon products without organic sulphur-containing component were observed with all catalysts under different operating conditions. The chlorine-containing and sulphur-containing products shown in the distribution of gaseous hydrocarbons are not detectable in this study. The mass and heteroatom balances in this paper are a matter still to be resolved fully, though it is clear that the missing material is not very high molecular weight material that is unreacted or deposited in the system. However, a catalyst system with both post-consumer polymer wastes and reaction conditions that has been used to address the recycling desire to see comparison with individual polymers further strengthens the interesting results of this research.

Polystyrene is known to degrade with an unzipping reaction to form mainly its monomer in pyrolysis reactions. However, this is not true for polyethylene or polypropylene for their degradation especially in the presence of acidic cracking catalysts. The major products of polystyrene cracking over various catalysts were styrene at about 4–5 wt.% with light aromatics (such as benzene, toluene, ethyl-benzene and xylenes, etc.) and smaller chain olefins and paraffins, and with some amount of unidentified products (unconverted polystyrene and coke formation over the reaction) deposited on the catalyst. The results from this work indicate that although the initial cracking of polymer waste must be confined to the external surface and pore mouths of the cracking catalysts, the resultant initial cracked products are then degraded further within the catalyst. In this paper, the residue deposited on the catalyst contained involatile products and coke, and their amounts were only determined by TGA. A fuller paper for the catalytic degradation of mixed polymer wastes is being developed from catalyst types and their deactivation behaviours in relation to coke formation and the kinetic/mechanistic model.

4. Conclusions

Polymer waste can cause serious pollution but also could be regarded as a cheap and abundant source of chemicals and energy. A laboratory catalytic fluidised-bed reactor has been used to obtain a range of volatile hydrocarbons by catalytic degradation of post-consumer polymer waste in the temperature range 290–430 °C. The catalytic degradation of commingled polymer mixture (PE/PP/PS/PVC) performed in fluidised-bed reactor was demonstrated to be a useful method for the production of potentially valuable hydrocarbons.

The acidic zeolite catalysts, HZSM-5, HMOR and HUSY, catalysed degradation resulted in much more amounts of volatile hydrocarbons compared with degradation over non-zeolitic catalysts (MCM-41 and SAHA). MCM-41 with large mesopores and SAHA with weaker acid sites resulted in a highly olefinic product and gave a wide carbon number distribution, whereas HUSY yielded a saturate-rich product with a wide carbon number distribution and substantial coke levels. Greater product selectivity was observed with HZSM-5 as catalysts with about 60% of the product in the C_3–C_5 range and HMOR generating the highest yield of butanes (C_4) for all catalysts studied. The larger pore zeolites (HUSY and HMOR) showed deactivation during the course of the degradation in contrast to the more restrictive HZSM-5. Observed differences in product yields and product distributions under identical reaction conditions can be attributed to the microstructure of catalysts.

The systematic experiments discussed in this paper show that the use of various catalysts improve the yield of volatile products and provide better selectivity in the product distributions. The selectivity could be further influenced by changes in reactor conditions; in particular, olefins and *iso*-olefins were produced by low temperatures and short contact times. It is concluded that under appropriate reaction conditions and suitable catalysts can have the ability to control both the product yield and product distribution from polymer degradation, potentially leading to a cheaper process with more valuable products.

References

[1] Recycling rates of Japan, US, and EU; Plastics production and waste discharge, PWMI Newsletter 26 (2003) 4, 8.
[2] M. Lee, Feedstock recycling: new plastic for old, Chem. Britain 31 (1995) 515.
[3] J. Brandrup, M. Bittner, W. Michaeli, G. Menges, Recycling Recovery of Plastics, Carl Hanser Verlag, Munich, New York, 1996.
[4] N. Billingham, Polymers the Environment, Gerald Scott, Royal Society of Chemistry, London, 1999.
[5] M. Kagayama, M. Igarashi, J. Fukada, D. Kunii, Thermal conversion of solid wastes and biomass, in: ACS Symposium Series, vol. 130, Washington, DC, 1980, p. 527.
[6] M. Igarashi, Y. Hayafune, R. Sugamiya, Y. Nakagawa, Pyrolysis of municipal solid waste in a fluidised reactor, J. Energy Resour. Technol. 106 (1984) 377.
[7] W. Kaminsky, B. Schlesselmann, C. Simon, Olefins from polyolefins and mixed plastics by pyrolysis, J. Anal. Appl. Pyrol. 32 (1995) 19.
[8] S. Hardman, S.A. Leng, D.C. Wilson, BP Chemicals Limited, Polymer Cracking, Eur. Patent Appl. 567 292 (1993).
[9] I. Fortelny, D. Michalkova, Z. Krulis, An efficient method of material recycling of municipal plastic waste, Polym. Degrad. Stab. 85 (2004) 975.
[10] W. Kaminsky, M. Predel, A. Sadiki, Feedstock recycling of polymers by pyrolysis in a fluidized bed, Polym. Degrad. Stab. 85 (2004) 1045.
[11] G. Audisio, F. Bertini, P.L. Beltrame, P. Carniti, Catalytic degradation of polyolefins, Makromol. Chem. Macromol. Symp. 57 (1992) 191.
[12] H. Ohkita, R. Nishiyama, Y. Tochihara, T. Mizushima, N. Kakuta, Y. Morioka, Y. Namiki, H. Katoh, H. Sunazyka, R. Nakayama, T. Kuroyanagi, Acid properties of silica–alumina catalysts and catalytic degradation of polyethylene, Ind. Eng. Chem. Res. 32 (1993) 3112.
[13] R.C. Mordi, R. Fields, J. Dwyer, Thermolysis of low density polyethylene catalysed by zeolites, J. Anal. Appl. Pyrol. 29 (1994) 45.
[14] Y. Sakata, M.A. Uddin, K. Koizumi, K. Murata, Catalytic degradation of polypropylene into liquid hydrocarbons using silica–alumina catalyst, Chem. Lett. (1996) 245.

[15] A.A. Garforth, Y.-H. Lin, P.N. Sharratt, J. Dwyer, Catalytic polymer degradation for producing hydrocarbons over zeolites, Stud. Surf. Sci. Catal. 21 (1999) 202.
[16] Y. Uemichi, J. Nakamura, T. Itoh, A.A. Garforth, J. Dwyer, Conversion of polyethylene into gasoline-range fuels by two-stage catalytic degradation using silica–alumina and HZSM-5 zeolite, Ind. Eng. Chem. Res. 38 (1999) 385.
[17] S.C. Cardona, A. Corma, Tertiary recycling of polypropylene by catalytic cracking in a semibatch stirred reactor; use of spent equilibrium FCC commercial catalyst, Appl. Catal. B 25 (2000) 151.
[18] J. Aguado, D.P. Serrano, M.D. Romero, J.M. Escola, Catalytic conversion of polyethylene into fuels over mesoporous MCM-41, Chem. Commun. (1996) 725.
[19] A. Dawood, K. Miura, Catalytic pyrolysis of γ-irradiated polypropylene over HY-zeolite for enhancing the reactivity and the product selectivity, Polym. Degrad. Stab. 76 (2002) 4525.
[20] J. Aguado, D.P. Serrano, J.M. Escola, E. Garagorri, J.A. Fernandez, Catalytic conversion polyolefins into fuels over zeolite beta, Polym. Degrad. Stab. 70 (2002) 97.
[21] A.R. Songip, T. Masuda, H. Kuwahara, K. Hashimoto, Kinetic studies for catalytic cracking of heavy oil from waste plastics over REY zeolite, Energy Fuels 8 (1994) 131.
[22] P.N. Sharratt, Y.-H. Lin, A. Garforth, J. Dwyer, Investigation of the catalytic pyrolysis of high density polyethylene over HZSM-5 catalyst in a laboratory fluidised bed reactor, Ind. Eng. Chem. Res. 36 (1997) 5118.
[23] Y.-H. Lin, P.N. Sharratt, A. Garforth, J. Dwyer, Catalytic conversion of polyolefins to chemicals and fuels over various cracking catalysts, Energy Fuels 12 (1998) 767.
[24] Y.-H. Lin, M.H. Yang, T.F. Yeh, M.D. Ger, Catalytic degradation of high density polyethylene over mesoporous and microporous catalysts in a fluidised-bed reactor, Polym. Degrad. Stab. 86 (2004) 121.
[25] J.S. Beck, D.C. Calabro, S.B. Mccullen, B.P. Pelrine, K.D. Schmitt, J.C. Vartuli, US Patent 5 145 816 (1992).
[26] Y.-H. Lin, Experimental and theoretical studies on the catalytic degradation of polymers, Ph.D. Thesis, UMIST, 1998.
[27] Y.-H. Lin, W.H. Hwu, M.D. Ger, T.F. Yeh, J. Dwyer, A combined kinetic and mechanistic modelling of the catalytic degradation of polymers, J. Mol. Catal. A: Chemical 171 (2001) 143.
[28] Y.-H. Lin, P.N. Sharratt, A.A. Garforth, J. Dwyer, Investigation of the deactivation of ultrastable Y zeolite by coke formation during the catalytic degradation of high density polyethylene, Thermochim. Acta 294 (1997) 45.